ELSEVIER

Int. J. Therm. Sci. 41 (2002) 41–49

International Journal of Thermal Sciences

Validity of solid-side mass diffusivity in simulation of water vapor adsorbed by silica gel in packed beds

Jung-Yang San, Cheng-Chin Ni, Sheng-Hsiang Hsu

Department of Mechanical Engineering, National Chung Hsing University, 250 Kuo-Kuang Road, Taichung, Taiwan ROC

Received 12 December 2000; accepted 22 February 2001

Abstract

Three different sets of solid-side mass diffusivity are individually used in simulation of the heat and mass transfer in a silica gel packed bed. The packed bed is installed at the exit of a fixed-bed dehumidification system to dampen the periodical moisture fluctuation. One of the three sets of solid-side mass diffusivity is experimental data. The other two, individually with a tortuosity factor (τ_s) of 1.0 and 2.8, are theoretical results in an Arrhenius form. The variations of air temperature and humidity ratio at the inlet and outlet of the packed bed are measured. The measured data match well with the simulation results obtained by using the measured D. The three sets of solid-side mass diffusivity are also individually used in simulation of the heat and mass transfer in a packed-bed dehumidification system in which the silica gel particles experience with a significant cyclic temperature variation. The validity of the two theoretical solid-side mass diffusivities is discussed for various operating conditions. The comparison shows that the computer simulation with τ_s of 1.0 predicts the processes more accurate than that with τ_s of 2.8 does.

Keywords: Adsorption; Mass diffusivity; Silica gel; Packed bed; Dehumidification

1. Introduction

Due to having a low utility cost and maintenance cost, packed beds are widely used in adsorption of water vapor, organic solvent and some toxic gases. The performance of a packed bed is significantly affected by the solid-side mass diffusivity of the adsorbate in the adsorbent, if the external fluid-film mass transfer resistance between the solid adsorbent and adsorbate is smaller or not much greater than the internal solid-side mass diffusion resistance. The solid-side mass diffusivity for an adsorbent to an adsorbate is a physical property. Strickly speaking, it needs to be determined from experimental measurement. Since the experiment for measuring solid-side mass diffusivity is sophisticated and time-consuming, for the sake of brevity, this property sometimes is directly obtained through theoretical approaches [1]. In doing so, computer simulations of adsorption processes will be convenient and useful, provided that its accuracy is acceptable.

Pesaran et al. [1,2] investigated the moisture transport in a silica gel packed-bed system with particular attention to solid-side resistance to moisture difference in the adsorbent particle. In their work, an Arrhenius form of solid-side mass diffusivity was proposed and a solid-side resistance model was developed for analyzing the heat and mass transfer process. Clark et al. [3] compared a set of experimental data to theoretical results for a thin silica gel packed bed. In the analysis, a gas-side controlled heat and mass transfer model incorporated a solid-side mass diffusion resistance was used. San et al. [4,5] applied the solid-side resistance model, which was originally proposed by Pesaran et al. [1, 2], in analyzing the adsorption performance of packed beds in a periodic steady-state operation.

In this work, two different operations of a silica gel packed bed are considered. One of the two operations treats the silica gel packed bed as a dehumidifier and the other treats it as a moisture damper. Fig. 1 shows the layout of a simple fixed-bed adsorption system. The fixed-bed adsorption system would be a packed-bed system if the two fixed beds are packed with adsorbent particles. A packed-bed system for dehumidification (states 1-8, Fig. 1) usually consists of two columns filled with a solid adsorbent. These two columns are arranged in a periodic switched operation. While one is for adsorption (states 10-11-1-3-7-8-9, Fig. 1), the other is for desorption (states 5-6-4-2-12). In order to proceed a cyclic operation, a regeneration heat is imposed

E-mail address: jysan@dragon.nchu.edu.tw (J.-Y. San).

1290-0729/02/$ – see front matter
PII: S1290-0729(01)01302-3

Nomenclature

$a_{1\text{-}3}$	coefficients defined by Eq. (8)	
A	bed cross-sectional area	m^2
$A_{1\text{-}9}$	coefficients defined by Eq. (2)	
A_s	total heat or mass transfer area	m^2
Bi_m	mass transfer Biot number $= K_G r_0/\rho_p D_{s,eff}$	
c	equilibrium water vapor concentration	$kg\cdot m^{-3}$
c_b	bed specific heat	$kJ\cdot kg^{-1}\cdot K^{-1}$
$c_{1\text{-}3}$	coefficients defined by Eq. (8)	
$c_{p,e}$	specific heat of humid air	$kJ\cdot kg^{-1}\cdot K^{-1}$
$c_{p,l}$	specific heat of water vapor	$kJ\cdot kg^{-1}\cdot K^{-1}$
C^*	mass ratio of silica gel to processed air $= \rho_b AL/\dot{m}_G\tau$	
D	solid-side mass diffusivity	$m^2\cdot s^{-1}$
D^*	non-dimensional surface mass diffusion coefficient $= D_{s,eff}\tau/r_0^2$	
D_0	constant $= 1.6\times10^{-6}$	$m^2\cdot s^{-1}$
D_s	surface mass diffusion coefficient	$m^2\cdot s^{-1}$
f	fluid friction coefficient	
h_c	convective heat transfer coefficient	$W\cdot m^{-2}\cdot K^{-1}$
H_{ads}	heat of adsorption	$kJ\cdot(kg\,H_2O)^{-1}$
K_G	gas-side mass transfer coefficient	$kg\cdot m^{-2}\cdot s^{-1}$
L	bed length	m
Le	overall Lewis number $= h_c/K_G c_{p,e}$	
m	bonding factor	
m_1	mass fraction of water vapor in humid air	$(g\,H_2O)\cdot(g\,air)^{-1}$
$\dot{m}_G$	mass flowrate of humid air	$kg\cdot s^{-1}$
Ntu	number of mass transfer unit $= K_G pL/\dot{m}_G$	
p	bed perimeter $= A_s/L$	m
r	radial coordinate	m
r^*	non-dimensional radial coordinate $= r/r_0$	
r_0	particle radius	m
R	gas constant	$kJ\cdot kg^{-1}\cdot K^{-1}$
Re	Reynolds number $= 2r_0V/\nu$	
t	time	s
t^*	non-dimensional time $= t/\tau$	
T	temperature	K
T^*	non-dimensional temperature $= T/T_{in}$	
V	bed inlet air velocity	$m\cdot s^{-1}$
W	moisture content	$(g\,H_2O)\cdot(g\,solid)^{-1}$
Y	humidity ratio	$(g\,H_2O)\cdot(g\,air)^{-1}$
z	axial coordinate	m
z^*	non-dimensional axial coordinate $= z/L$	

Greek symbols

α	function of W and T
γ_1	$c_{p,l}/c_{p,e}$
γ_2	$c_{p,e}/c_b$
γ_3	$H_{ads}/(c_b T_{in})$
ν	kinematic viscosity $\cdots$ $m^2\cdot s^{-1}$
ρ	density $\cdots$ $kg\cdot m^{-3}$
σ	non-dimensional length factor
τ	half cycle period $\cdots$ s
τ_s	tortuosity factor of pore path

Subscripts

0	initial value
ads	adsorption
b	packed bed
des	desorption
e	ambient
eff	effective
in	inlet
p	particle
s	adsorbent surface

on the adsorbent in desorption mode (states 5-6). The above system can effectively reduce the overall humidity ratio of processed air. Nevertheless, the humidity ratio at the exit of the system is time-varying. This is oftenly unfavorable to industrial applications if the fluctuation is significant. To avoid this disadvantage, an additional packed bed (states 8-9, Fig. 1) can be used as a moisture damper to reduce the amplitude of this fluctuation. Basically, the heat and mass transfer in a moisture damper is very similar to that in a packed-bed dehumidifier. The main difference is that the temperature variation of the adsorbent in the latter is much greater than that in the former. In this work, the heat and mass transfer in a packed-bed dehumidifier and the heat and mass transfer in a moisture damper are individually analyzed by using a computer program with three different sets of solid-side mass diffusivity. One of the three sets of data is experimentally determined and the other two are theoretically developed. The time-varying air temperature and humidity ratio at the inlet and outlet of the moisture damper are measured. The simulation results are compared with the measured data to check the validity of the two sets of theoretical solid-side mass diffusivity.

2. Mathematical model

Pesaran et al. [1] proposed a solid-side resistance model to predict the transient heat and mass transfer in a thin silica gel packed bed. This model was modified by San et al. [4] by considering the fluid friction effect for simulation

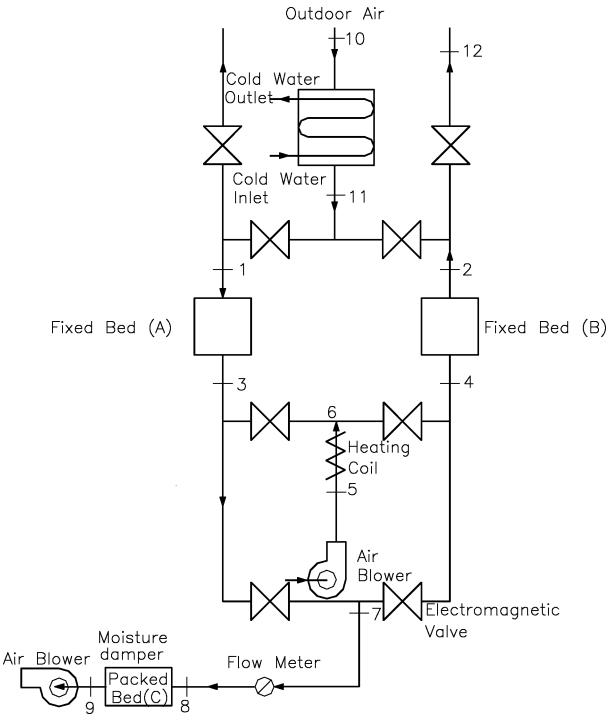

Fig. 1. A fixed-bed dehumidification system with a moisture damper.

of the process in a thick packed bed. In this analysis, this modified model is used to investigate the effects of solid-side mass diffusivity on the heat and mass transfer for water vapor adsorbed by a regular density silica gel. The governing equations of this modified model can be expressed as follows:

(I) Mass diffusion in the particle:

$$\frac{\partial W}{\partial t^*} = \frac{1}{r^{*2}}\frac{\partial}{\partial r^*}\left(r^{*2}D^*\frac{\partial W}{\partial r^*}\right) \tag{1}$$

initial condition:

$$W\left(r^*, z^*, t^* = 0\right) = W_0\left(r^*, z^*\right)$$

boundary conditions:

$$\left.\frac{\partial W}{\partial r^*}\right|_{r=0} = 0$$

$$\left.\frac{\partial W}{\partial r^*}\right|_{r=1} = -Bi_m(m_{1,\mathrm{s}} - m_{1,\mathrm{e}})$$

(II) Equilibrium isotherms of silica gel [6]:

$$W(c,T) = A_1 + A_2T + A_3T^2 + A_4c + A_5c^2 + A_6Tc + A_7T^2c + A_8Tc^2 + A_9T^2c^2 \tag{2}$$

where

(i) for $W < 0.05$:

$$A_1 = 8.98\times10^{-3},\quad A_2 = -5.15\times10^{-4}$$
$$A_3 = 6.04\times10^{-6},\quad A_4 = 4.39\times10^{2}$$
$$A_5 = -1.07\times10^{5},\quad A_6 = -1.13\times10^{1}$$
$$A_7 = 7.45\times10^{-2},\quad A_8 = 2.97\times10^{3}$$
$$A_9 = -2.05\times10^{1}$$

(ii) for $0.05 \leqslant W \leqslant 0.3$:

$$A_1 = 0.22807,\quad A_2 = -6.02\times10^{-3}$$
$$A_3 = 4.50\times10^{-5},\quad A_4 = 5.32\times10^{1}$$
$$A_5 = -9.84\times10^{2},\quad A_6 = -1.1084$$
$$A_7 = 5.81\times10^{-3},\quad A_8 = 2.58\times10^{1}$$
$$A_9 = -0.16933$$

(iii) for $W > 0.3$:

$$A_1 = 0.40416,\quad A_2 = -0.77\times10^{-2}$$
$$A_3 = 4.16\times10^{-5},\quad A_4 = 2.28\times10^{1}$$
$$A_5 = -3.27\times10^{2},\quad A_6 = -0.39024$$
$$A_7 = 0.15\times10^{-2},\quad A_8 = 8.1546$$
$$A_9 = -5.11\times10^{-2}$$

(III) Mass transfer of water vapor in the air stream:

$$\frac{\partial m_{1,\mathrm{e}}}{\partial z^*} = Ntu(m_{1,\mathrm{s}} - m_{1,\mathrm{e}})(1 - m_{1,\mathrm{e}}) \tag{3}$$

boundary condition:

$$m_{1,\mathrm{e}}\left(z^* = 0, t^*\right) = m_{1,\mathrm{in}}$$

(IV) Energy balance in the air stream:

$$\frac{\partial T_{\mathrm{e}}^*}{\partial z^*} = Ntu\left[Le\left(T_{\mathrm{s}}^* - T_{\mathrm{e}}^*\right) + \left(\gamma_1 T_{\mathrm{s}}^* - T_{\mathrm{e}}^*\right) \times (m_{1,\mathrm{s}} - m_{1,\mathrm{e}}) + \sigma\left(fRe^2\right)\right] \tag{4}$$

boundary condition:

$$T_{\mathrm{e}}^*\left(z^* = 0, t^*\right) = 1.0$$

(V) Energy balance in the solid:

$$\frac{\partial T_{\mathrm{s}}^*}{\partial t^*} = \frac{Ntu}{C^*}\left[Le\gamma_2\left(T_{\mathrm{e}}^* - T_{\mathrm{s}}^*\right) - \gamma_3(m_{1,\mathrm{s}} - m_{1,\mathrm{e}})\right] \tag{5}$$

initial condition:

$$T_{\mathrm{s}}^*\left(z^*, t^* = 0\right) = T_0/T_{\mathrm{in}}$$

Knudsen diffusion, ordinary diffusion and surface diffusion are three major mechanisms affecting the mass diffusion rate of an adsorbate in an adsorbent. It had been verified [1], for water diffusing in a regular density silica gel, both the Knudsen diffusion and ordinary diffusion can be neglected. Thus in this work only the surface mass diffusion is considered. In the above governing equations, Eq. (2) represents the equilibrium isotherms of silica gel in adsorption of water vapor. This set of data was measured in a previous work [6]. In Eq. (4), σ is a non-dimensional length factor. Its detailed expression can be found in reference [4].

Eqs. (1)–(5) are numerically solved to simulate the cyclic operation of packed beds. A Crank–Nicholson scheme is used for solving Eq. (1) and a fourth-order Runge–Kutta scheme is used for solving the rest equations. In solving the above governing equations, the cyclic mass balance of adsorbate in the solid is an important factor indicating the accuracy of the solution. If the mass balance is poor, an increase of the computational nodes in the r^* axis and z^* axis is necessary.

3. Solid-side mass diffusivity

3.1. Theoretical prediction

Sladek et al. [7] proposed a simple Arrhenius-form equation to estimate the surface mass diffusion coefficient. This equation can be expressed as follows:

$$D_s = D_0 \exp\left[-(0.45/m)(H_{ads}/RT)\right] \tag{6}$$

where D_0 equals 1.6×10^{-6}, H_{ads} is the heat of adsorption, R is the gas constant and m is a constant relating to the type of bond between adsorbate and adsorbent. Eq. (6) was used by Pesaran et al. [1] to simulate the heat and mass transfer for silica gel in adsorption of water vapor from humid air in a packed bed. In Pesaran's work, the tortuosity of pore path was considered and the value of m was selected as 1.0. If so, Eq. (6) can be expressed as follows:

$$D_{s,\text{eff}} = D_s/\tau_s = (D_0/\tau_s)\exp(-0.974H_{ads}/T) \tag{7}$$

In the above equation, τ_s is the tortuosity factor which, as suggested by Pesaran et al. [1], equals 2.8 for regular-density silica gels. As mentioned earlier, for regular-density silica gels, both the Knudsen diffusion and ordinary diffusion can be neglected. Thus the above surface mass diffusion coefficient ($D_{s,\text{eff}}$) is recognized as the solid-side mass diffusivity (D).

3.2. Experimental data

A set of solid-side mass diffusivity for a regular-density silica gel particle with a diameter of 1.5 mm is used for comparison in this analysis [6]. The set of data was measured by using a traditional thermal-gravimetrical method. In the measurement, a certain amount of the silica gel particle was uniformly placed on a stainless steel screen in a vacuum chamber for dehydration. The vacuum chamber was embedded in a water bath to control the equilibrium temperature of the adsorption process. The stainless steel screen was seated on a miniature load cell. After the dehydration was complete, the dry weight of the silica gel particles was measured. Then a steady low humidity air, which was set at the same temperature as that of the water bath, was arranged to pass through the chamber. During the adsorption, the weight of the wet silica gel particles was dynamically recorded, thus the uptake curve for the silica gel-water vapor system at this specific temperature and humidity ratio was obtained. After the adsorption was complete, the adsorbed water in the silica gel particles was in equilibrium with the water vapor in the air. At this moment, by arranging a small step increase of air humidity ratio, another uptake curve at this new humidity ratio was obtained. In the work, a previously derived adsorption model which considers both the thermal effect and external fluid-film mass transfer resistance was used [8] to evaluate the theoretical uptake curves. By matching the measured uptake data to its corresponding theoretical uptake curve, it yielded the solid-side mass diffusivity. The experiment was repeated for several temperatures. In doing so, the temperature dependency of the solid-side mass diffusivity was also obtained. The obtained solid-side mass diffusivities were originally correlated by using a fourth-order polynomial. This set of experimental data can also be correlated with an Arrhenius-form equation as follows:

$$D = D_0 \exp\left[-\alpha(H_{ads}/RT)\right] \tag{8}$$

where

$$\alpha(W,T) = \frac{a_3W^2 + a_2W + a_1}{c_3T + c_2 + (c_1/T)}$$

$$a_1 = 2.48, \qquad a_2 = 7.2, \qquad a_3 = -12.0$$

$$c_1 = 3.97, \qquad c_2 = -2.41 \times 10^{-2}$$

$$c_3 = 4.79 \times 10^{-5}$$

Eq. (8) is in a form similar to that of Eq. (6). In Eq. (8), α can be treated as the bonding factor between the adsorbent and adsorbate. This factor, no longer to be a constant as that in Eq. (6), instead it is a function of W and T. The theoretical solid-side mass diffusivity ($\tau_s = 1.0$) and the measured solid-side mass diffusivity are individually shown in Fig. 2. The comparison shows that the measured data are

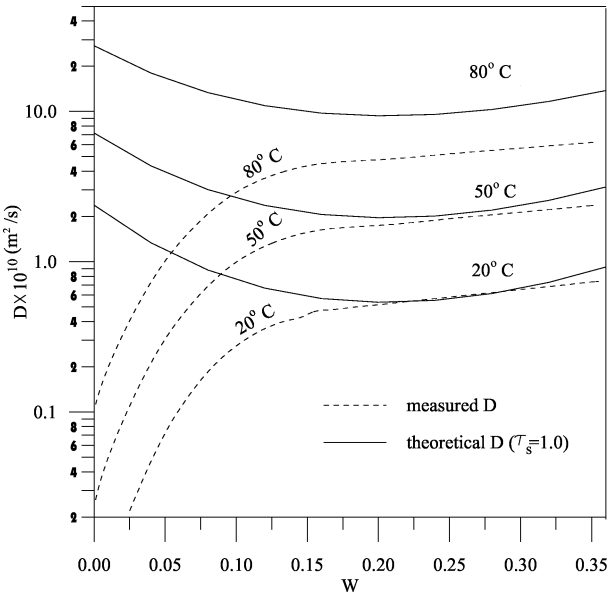

Fig. 2. Comparison between measured D and theoretical D.

greater than the theoretical results. The deviation between the two solid-side mass diffusivities is quite prominent at a small W. At a small W, the theoretically predicted solid-side mass diffusivity increases dramatically with the W. On the contrary, the measured solid-side mass diffusivity decreases with increasing the W. As interpreted by Gilliland et al. [9], the diffusion mechanism of molecules adsorbed on an adsorbent at a small W is different from that at a large W. At a small W, a discrete hopping theory for adsorbed molecules is adequate to explain migration of molecules. In other words, adsorbed molecules hop between adjacent adsorption sites. As the W increases, self-encounters of migration molecules would also increase. This results in a decrease of the solid-side mass diffusivity. At a large W, a self-diffusion theory for ordinary liquid should be used to interpret the diffusion mechanism. For a large W, since migration of molecules on the second layer is less bound than those on the monolayer. The solid-side mass diffusivity would increase with the W. Kruckels [10] studied the surface diffusion in the submonolayer concentration region for a regular-density silica gel in adsorption of water vapor. In his results, the mass diffusivity was found to decrease with an increase of the W. The set of data indicated by Eq. (8) shows the same trend as Kruckels' results in the submonolayer region. In the multilayer region, this set of data fulfills the self-diffusion theory for ordinary liquid. Thus for $W < 0.18$, the D decreases with increasing the W; however, for $W > 0.18$, the D increases with the W. As indicated in Fig. 2, the theoretical D fails to satisfy the above discrete hopping theory for a small W.

The theoretical solid-side mass diffusivity in Fig. 2 has a tortuosity factor of 1.0. Eq. (7) has shown that the magnitude of tortuosity factor is inversely proportional to the theoretical solid-side mass diffusivity. As mentioned earlier, the tortuosity factor suggested by Pesaran et al. [1] is 2.8. If this value, 2.8, is used in evaluation of the solid-side mass diffusivity, the deviation between the measured D and theoretical D will be even greater than that shown in Fig. 2. Actually, Eq. (6) originally proposed by Sladek [7] was based on a set of experimental data for various adsorption systems. The effect of pore's tortuosity on the solid-side mass diffusion is already considered in its expression. Thus, an additional tortuosity factor, 2.8, imposed on Eq. (7) would result in an underestimation of the magnitude of solid-side mass diffusivity.

4. Temperature and humidity measurement

In this work, a silica gel packed bed (states 8-9, Fig. 1) is installed at the exit of a fixed-bed solid desiccant dehumidification system to dampen the humidity fluctuation of processed air. The fixed-bed system does not contain two packed beds. Instead, it is composed of two identical honeycomb type dehumidifiers (250 mm in diameter and 400 mm in thickness) which are impregnated with silica gel. The schematic of the system is shown in Fig. 1. As shown in the diagram, the volumetric flowrate of processed air is measured by using a rotameter-type flowmeter. The cyclic temperature variations at states 8 and 9 are individually measured by using a T-type thermocouple with a bead diameter less than 0.25 mm. The cyclic dewpoint temperature variations at these two states are individually measured by using a dewpoint temperature hygrometer (Rotronics, M-DP05). The signals of thermocouples and hygrometers are picked up by a data recorder (Yokogawa, HR-1300). The measured data are compared to the computer simulation results to check the validity of the considered solid-side mass diffusivities. In this experiment, the diameter of the packed bed is 250 mm. The volumetric flowrate of processed air is 1 $m^3 \cdot min^{-1}$. Two different bed lengths, 5 cm and 15 cm, are individually tested. The silica gel particle used in the moisture damper is the same as that considered in the previous diffusing rate measurement [6].

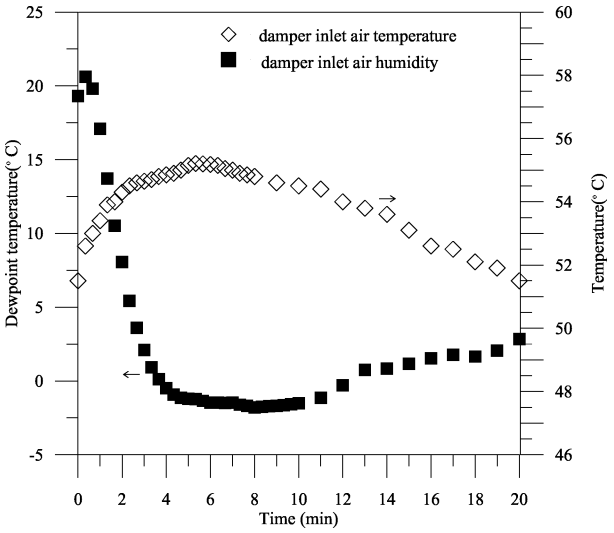

Fig. 3. Inlet air humidity and temperature of moisture damper in case (i).

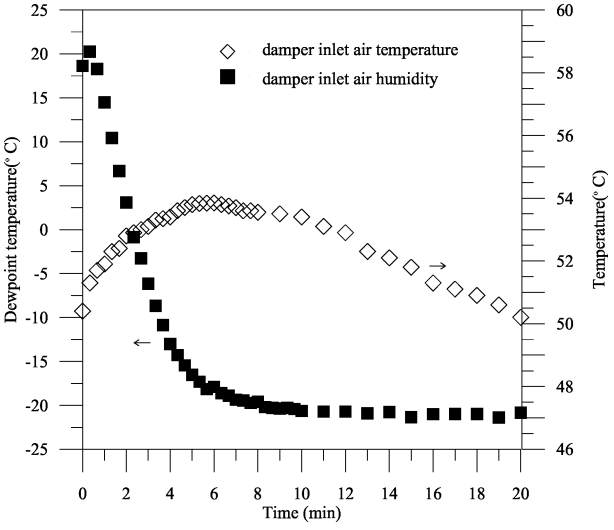

Fig. 4. Inlet air humidity and temperature of moisture damper in case (ii).

Two different sets of inlet air humidity and temperature for the moisture damper are considered. One corresponds to a high inlet air humidity condition which results from the operation of the dehumidification system without a cooling coiler (states 10-11 in Fig. 1); the other corresponds to a low inlet air humidity condition which results from the operation with a cooling coiler. Fig. 3 represents the measured data for the former (case (i)) and Fig. 4 shows that for the latter (case (ii)).

5. Results

The experimental data represented in Fig. 5 illustrate the damping effect of the packed bed (states 8-9 in Fig. 1). As shown in the diagram, the fluctuation of dewpoint temperature at state 8 varies from 22 °C to −20 °C in a cyclic period of 20 minutes. After the flow passing through the packed bed, the fluctuation of dewpoint temperature reduces and it varies in the range of 0 °C to −12 °C. This indicates that the packed bed is quite effective to act as a moisture damper. Fig. 5 also indicates that, in the first 5 minutes of the cyclic period the bed is in adsorption and in the next 15 minutes it is in desorption.

Fig. 6 shows three sets of simulation results and one set of experimental data for the air humidity ratio at state 9. The corresponding air humidity and temperature at state 8 are shown in Fig. 3 (case (i)). The simulation result obtained by using the measured solid-side mass diffusivity shows a smaller deviation to the experimental data; the other two simulation results obtained by using the theoretical D reveal a larger deviation to the experimental data. If the comparison is made between the two simulation results obtained by using the theoretical D, the one with τ_S of 1.0 appears to match with the experimental data better than the other with τ_S of 2.8 does. However, in either case, the deviation mainly occurs in the initial stage of the process. As shown in Fig. 2, the measured D is greater than the two theoretical D and its deviation increases with decreasing the W. For the two cases using the theoretical D, the increasing rate of moisture concentration on the surface of silica gel particles is much greater than that using the measured D. Thus the rise of the exit air humidity ratio at state 9 (in the first one or two minutes of the process) for the two cases using the theoretical D occurs earlier than that for the case using the measured D.

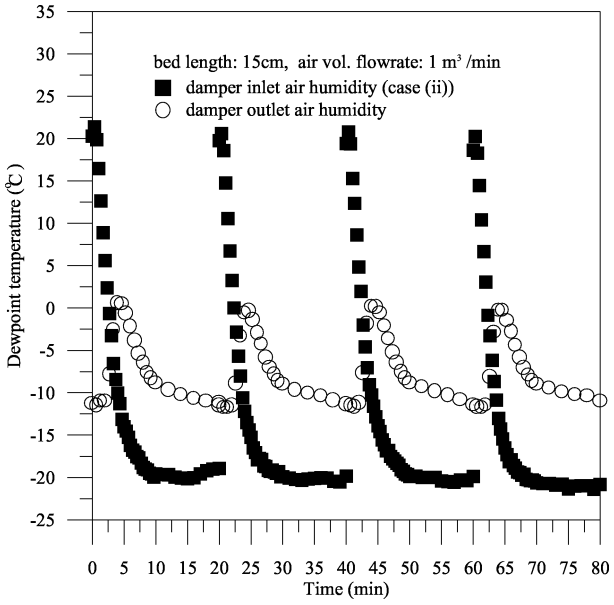

Fig. 5. Performance of a moisture damper.

Fig. 7 shows a similar result as that shown in Fig. 6. Since the bed length of the moisture damper in Fig. 7 is three times of that in Fig. 6, the fluctuation of exit air humidity ratio is reduced and the occurrence of the maximum dewpoint temperature is postponed. Due to the same reason as that in Fig. 6, the rise of exit air humidity ratio for the two cases

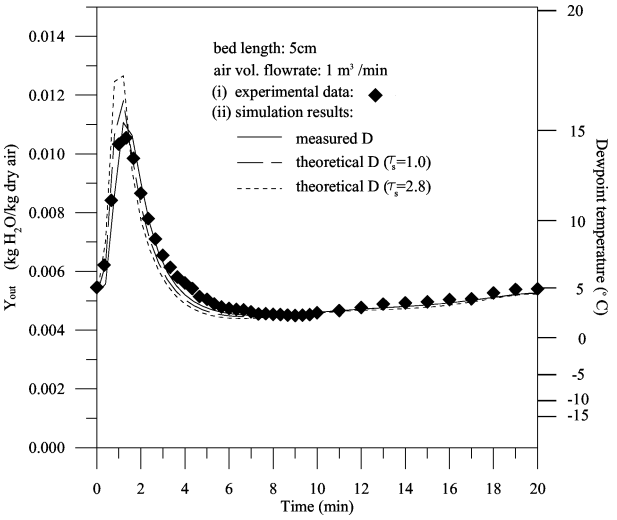

Fig. 6. Outlet air humidity ratio of a moisture damper with a bed length of 5 cm (case (i)).

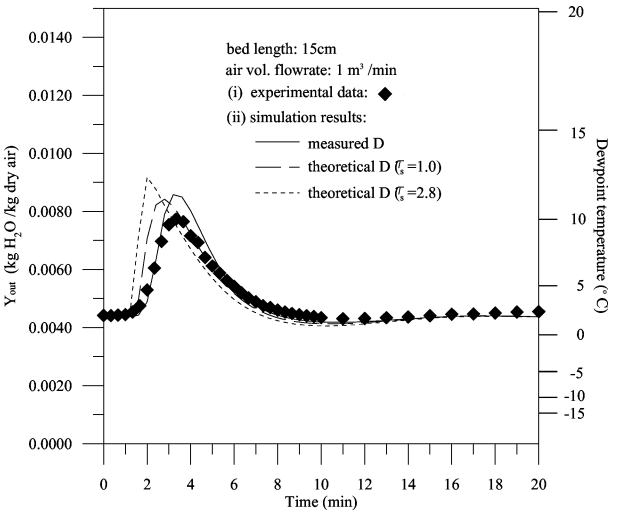

Fig. 7. Outlet air humidity ratio of a moisture damper with a bed length of 15 cm (case (i)).

using the theoretical D occurs earlier than that for the case using the measured D.

Fig. 8 represents three sets of simulation results and one set of experimental data for the air humidity ratio at state 9. The corresponding air humidity and temperature at state 8 are shown in Fig. 4 (case (ii)) and the considered bed length is 5 cm. As illustrated in Fig. 8, the discrepancy between the experimental data and the simulation results obtained by using the theoretical D is quite prominent in the initial stage of the process. Compared the deviation of the results in Fig. 8 to that in Fig. 6, it clearly shows that the former is more significant than the latter. The inlet air humidity ratio for the considered case in Fig. 8 is much lower than that in Fig. 6. Thus in the beginning of the process, the solid-side mass diffusion in Fig. 8 occurs at a W much lower than that in Fig. 6. As mentioned earlier, the deviation between the theoretical D and measured D increases with decreasing the W. Thus the deviation in Fig. 8 is larger than that in Fig. 6.

Fig. 9 shows the simulation results and experimental data for a moisture damper with a bed length of 15 cm. As indicated in the diagram, the case using the measured D still matches well with the experimental data. Compared the results in Fig. 9, to those in Fig. 8, it may find that, for an increase of the bed length, the fluctuation of exit air humidity ratio is reduced and the occurrence of the maximum dewpoint temperature is postponed.

In this work, the measured D and the two sets of theoretical D are also individually used in simulation of the adsorption process for a packed-bed dehumidification system. The length of the bed is 15 cm and its diameter is 25 cm. Figs. 10–12 illustrate the dewpoint temperature of processed air at the exit of the packed-bed dehumidification system (state 7 in Fig. 1) in a periodic steady-state operation. In Fig. 10, the adsorption time period (half cycle time) is 20 minutes. The three curves in the diagram individually represent the simulation results obtained by using the three different sets of D as considered in Fig. 9. The comparison shows that, except in the initial stage of the process, the three curves basically are different. In the initial stage of the process, the temperature of the silica gel particles in the packed bed is quite high. Instead of the moisture content (W), the temperature drop of the silica gel particles actually dominates the adsorption performance. The rates of temperature drop for the three considered cases are almost the same. Thus in the initial stage of the process (less than 4 minutes), the three curves are quite similar. After the temperature of the silica gel particles drops to a certain degree, the moisture content starts to play an important role in the process. As mentioned earlier, if the D is small, the solid-side mass diffusion resistance would be large. Consequently, during the adsorption mode, the increasing rate of water concentration on the surface layer of adsorbent ($r = r_0$) will also be large and thus the adsorption rate

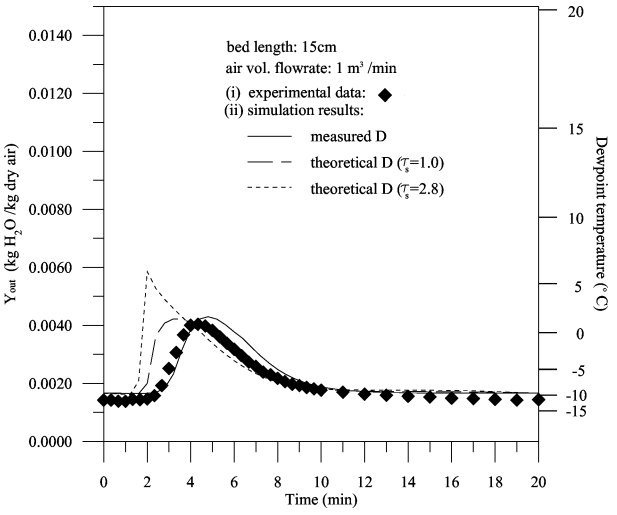

Fig. 9. Outlet air humidity ratio of a moisture damper with a bed length of 15 cm (case (ii)).

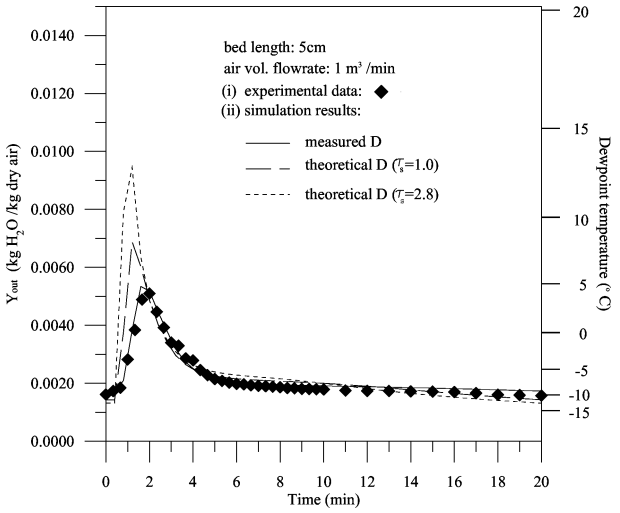

Fig. 8. Outlet air humidity ratio of a moisture damper with a bed length of 5 cm (case (ii)).

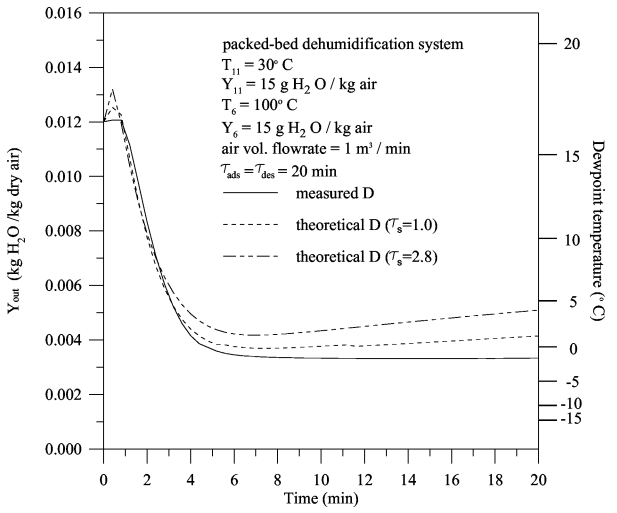

Fig. 10. Exit air dewpoint temperature ($Y_{11} = 15$ (g H_2O)·(kg air)$^{-1}$ and $\tau_{ads} = 20$ min).

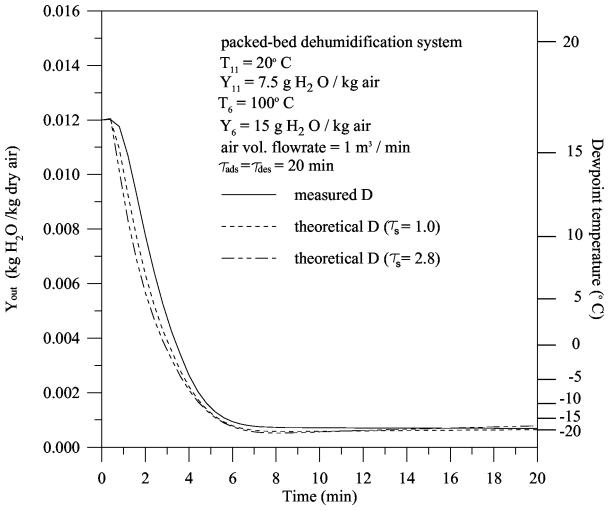

Fig. 11. Exit air dewpoint temperature ($Y_{11} = 7.5$ (g H_2O)·(kg air)$^{-1}$ and $\tau_{ads} = 20$ min).

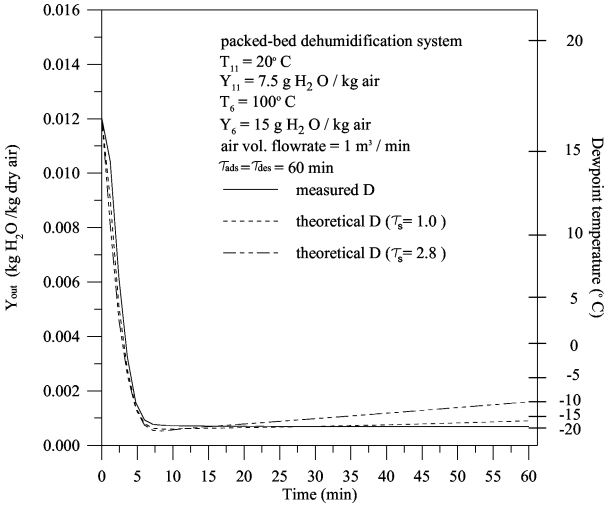

Fig. 12. Exit air dewpoint temperature ($Y_{11} = 7.5$ (g H_2O)·(kg air)$^{-1}$ and $\tau_{ads} = 60$ min).

will be small. As demonstrated earlier, the measured D is larger than the two sets of the theoretical D. This implies that the corresponding solid-side mass diffusion resistance for the case using the measured D is smaller than those using the theoretical D. This makes a larger adsorption rate for the case using the measured D. Thus it turns out that the dewpoint temperature of processed air would keep unchanged till the end of adsorption mode.

The considered inlet humidity ratio of processed air in Fig. 11 is much lower than that as considered in Fig. 10. Since the operating period is short, the adsorption performance predicted by using the measured D becomes slightly lower than the other two cases using the theoretical D. However, the deviation is very small. Similar to the case considered in Fig. 10, in the beginning of the adsorption process, the temperature of the silica gel particles is very high. As the processed air passing through the front of the packed bed, its temperature increases and its humidity ratio drops. However, as this hot and dry air flowing into the rear of the packed bed, it starts to regenerate the encountered silica gel particles. This phenomenon is especially pronounced for the case with a large D. Thus it results in a degradation of the adsorption performance in the initial stage of the process for the case using the measured D. In Fig. 11, the considered inlet air humidity ratio in the desorption (regeneration) mode is much higher than that in the adsorption mode. Thus the above phenomenon exists. In Fig. 10, the considered inlet air humidity ratio in the adsorption mode is the same as that in the desorption mode, thus this phenomenon can not be observed. Fig. 12 shows the predicted adsorption performance for the operation with a half cycle time of 60 minutes. For this operating condition, the predictions of the three cases are quite different. The cycle time in Fig. 11 is three times of that in Fig. 10. Thus in the final stage of the process, the surface of the silica gel particles for the two cases with the theoretical D starts to be saturated. It turns out that the adsorption performance predicted by using the measured D is better than the other two cases obtained by using the theoretical D. Based on the results indicated by Figs. 10, 11 and 12, it may conclude that, as long as the operating cycle time is short and the inlet humidity ratio of processed air is lower than that of regenerative air, the result obtained by using the theoretical D would be quite close to that obtained by using the measured D.

6. Conclusions

For the moisture damper, the exit air humidity ratio obtained from the computer simulation using the measured D matches well with the experimental data. For $W > 0.15$, the deviation between the measured D and the theoretical D ($\tau_s = 1.0$) is not significant; for $W < 0.15$, this deviation increases with decreasing the W. This results in a discrepancy of the exit air humidity ratio between the experimental data and the simulation results obtained by using the theoretical D. This discrepancy increases with decreasing the inlet air humidity. In order to improve the match, a modification of the theoretical Arrhenius-form solid-side mass diffusivity to fulfill the discrete hopping theory for migration of molecules in the low W region is required.

A cyclic variation of humidity ratio for the processed air at the exit of the moisture damper is observed. In the cycle, there exists a maximum air humidity ratio. An increase of the bed length reduces the deviation between the maximum air humidity ratio in the experimental data and the maximum air humidity ratio in the simulation results obtained by using the theoretical D. However, an increase of the bed length would enlarge the deviation on the corresponding time of the maximum air humidity ratio. The predicted exit air humidity ratio with τ_s of 1.0 matches the experimental data better than that with τ_s of 2.8 does. Generally speaking, as long as the bed is thin and the inlet air humidity ratio is not too low, the

simulation result with τ_s of 1.0 still assures the prediction with a certain degree of accuracy.

Using the theoretical D to simulate the process of the packed-bed dehumidification system might result in an underestimation of the adsorption performance. However, in the initial stage of the process, the exit air humidity predicted by using the theoretical D would appear quite close to that obtained by using the measured D. But in the final stage of the process, the deviation could be quite significant. If the operating cycle time is short and the inlet humidity ratio of processed air is lower than that of regenerative air, the entire result predicted by using the theoretical D will be close to that obtained by using the measured D.

References

[1] A.A. Pesaran, A.F. Mills, Moisture transport in silica gel packed beds—I, Internat. J. Heat Mass Transfer 30 (1987) 1037–1049.
[2] A.A. Pesaran, A.F. Mills, Moisture transport in silica gel packed beds—II, Internat. J. Heat Mass Transfer 30 (1987) 1051–1060.
[3] J.E. Clark, A.F. Mills, H. Buckberg, Design and testing of thin adiabatic desiccant beds for solar air conditioning applications, J. Solar Energy Engrg. 103 (1982) 89–91.
[4] J.Y. San, G.D. Jiang, Modeling and testing of a silica gel packed-bed system, Internat. J. Heat Mass Transfer 37 (1994) 1173–1179.
[5] J.Y. San, Y.C. Hsu, L.J. Wu, Adsorption of toluene on activated carbon in a packed bed, Internat. J. Heat Mass Transfer 41 (1998) 3229–3238.
[6] J.Y. San, Damping effect of a moisture capacitor in a fixed-bed solid desiccant dehumidification system, Nat. Sci. Council Report-Taiwan NSC89-2212-E-005-016 (2000) (in Chinese).
[7] K.J. Sladek, E.R. Gilliland, R.F. Baddour, Diffusion on surfaces. II. Correlation of diffusivities of physically and chemically adsorbed species, Industrial Engrg. Chemistry: Fundamentals 13 (1974) 100–105.
[8] C.C. Ni, J.Y. San, Mass diffusion in a spherical microporous particle with thermal effect and gas-side mass transfer resistance, Internat. J. Heat Mass Transfer 43 (2000) 2129–2139.
[9] E.R. Gilliland, R.F. Baddour, G.P. Perkinson, K.J. Sladek, Diffusion on surfaces. I. Effect of concentration on the diffusivity of physically adsorbed gases, Industrial Engrg. Chemistry: Fundamentals 13 (1974) 95–99.
[10] W.W. Kruckels, On gradient dependent diffusivity, Chemical Engrg. Sci. 28 (1973) 1565–1576.